Advances in Applied Mathematics and Mechanics
Adv. Appl. Math. Mech., Vol. **6**, No. 1, pp. 49-74

DOI: 10.4208/aamm.12-m1282
February 2014

On the Computations of Gas-Solid Mixture Two-Phase Flow

D. Zeidan[1,*] and R. Touma[2]

[1] *Department of Mathematics, Al-Balqa Applied University, Al-Salt, Jordan*
[2] *Department of Computer Science & Mathematics, Lebanese American University, Beirut, Lebanon*

Received 23 May 2012; Accepted (in revised version) 24 May 2013

Available online 13 December 2013

Abstract. This paper presents high-resolution computations of a two-phase gas-solid mixture using a well-defined mathematical model. The HLL Riemann solver is applied to solve the Riemann problem for the model equations. This solution is then employed in the construction of upwind Godunov methods to solve the general initial-boundary value problem for the two-phase gas-solid mixture. Several representative test cases have been carried out and numerical solutions are provided in comparison with existing numerical results. To demonstrate the robustness, effectiveness and capability of these methods, the model results are compared with reference solutions. In addition to that, these results are compared with the results of other simulations carried out for the same set of test cases using other numerical methods available in the literature. The diverse comparisons demonstrate that both the model equations and the numerical methods are clear in mathematical and physical concepts for two-phase fluid flow problems.

AMS subject classifications: 76T15, 76N10, 35L65, 65M08

Key words: Hyperbolic conservative equations, two-phase flows, compressible gas-solid, mixture conservation laws, approximate Riemann solver, upwind Godunov methods, numerical simulation.

1 Introduction

For many years the subject of theoretically modelling multi-phase fluid flows has held a prominent place in the attention of applied and computational mathematicians. In more recent years this attention has been directed to the well-defined mathematical models along with numerical methods. The basic issues in the subject traditionally deal with

*Corresponding author.
Email: dia@bau.edu.jo, diazeidan@gmail/yahoo.com (D. Zeidan)

hyperbolic or non-hyperbolic character of the governing equations, and conservative or non-conservative character of the governing equations. Typically, two-phase flow seen in a broad range applications and encompasses many different physical processes. It is therefore not possible for a single theoretical framework to describe all the diverse variety of two-phase fluid flow problems. The variety of two phase systems is illustrated by the different mathematical models suggested in the literature. In general, they are usually described by the two-fluid six equations model [4, 5, 11, 30, 31], or the mixture three equations model [14, 19], or the five equations model [13, 15], or the seven equations model [1, 27]. The success of each model depends on the physical phenomena of interest and on the nature of the problem. Almost all these models have non-conservative form causing serious analytical and numerical difficulties. Furthermore, hyperbolicity of such models is obtained under certain restrictions. Recently, an alternative approach based on the theory of thermodynamically compatible systems of hyperbolic conservation laws [7] to model two-phase flows has been proposed (see, for example, [23, 42]). For such an approach, the formulation of thermodynamically compatible systems have been applied to model two-phase gas-liquid [24,42] and gas-solid mixtures [25,46] in terms of parameters of state for the mixture. Distinctive features of this approach are that the resulting models admit two pressures, two velocities and two temperatures. Furthermore, the resulting models are fully hyperbolic and fully conservative systems of the governing equations and independent of the kind of numerical method used to implement it. As regard to the numerical tools for the simulation of two-phase flow equations, there are several numerical methods have been proposed in the literature from different perspectives to simulate two-phase flow problems. The details of these numerical methods are very well documented in the literature and not repeated here to which we will refer the reader to the recent papers [2, 6, 10, 12, 17, 18, 29, 34, 37, 40, 44, 47] and references therein for details.

This paper is to continue the present authors investigation in applying advanced numerical methods to solve thermodynamically compatible systems of hyperbolic conservation laws in the context of two-phase fluid flow problems. In a recent study [46], a mathematical model was developed for compressible gas-solid two-phase flow based on the thermodynamically compatible systems theory [7]. Theoretical investigation has shown that the model is fully hyperbolic and fully conservative with a complete mathematical structure of the governing equations. As a consequence, the model equations allows a straightforward application of finite volume methods and corresponding numerical tools. Thus, rather than developing new numerical methods specific to the two-phase flow model of this paper, we propose to adapt a general purpose method for hyperbolic systems of conservation laws that can be applied to the model equations. In earlier studies [23, 24, 42, 43], modern numerical methods such as Godunov methods of centred type were extended to thermodynamically compatible systems of conservation laws in the context of two-phase flow models.

The principal contribution of this paper is to extend and apply the well tested upwind Godunov methods directly to the model of two-phase gas-solid mixture developed in [46]. These methods are usually based on the exact or approximate solution of the local

Riemann problem for the constructions of the numerical fluxes. Within the framework of the Riemann problem, closed form solutions are limited and have been developed to certain two-phase flow models of the non-hyperbolic non-conservative type. See for example [3, 28, 32]. Thus, approximate Riemann solvers become practically popular for the solution of the local Riemann problem for such models. Moreover, an enormous amount of work has appeared on the subject of Riemann solvers for the constructions of the numerical fluxes and has been presented and successfully applied to several two-phase flow problems, to name but a few (see [21,26,34,36], and references therein, for further details). For the present model the exact solution of the Riemann problem is not available at this time for the types of equations of state involved for the phases as well as the mixture. Due to the complexity of the equations of state, approximate Riemann solvers are considered instead. One of the more commonly used Riemann solvers is the HLL Riemann solver (after Harten, Lax and van Leer) [9]. This solver is chosen for its simplicity, efficiency and as a starting point for investigations which should lead to suitable theoretical and numerical analysis for the current two-phase flow model. It is noteworthy that the HLL Riemann solver has also been used for other two-phase flow models of the non-hyperbolic non-conservative type, see [8, 22, 27, 39, 41], for example. The HLL Riemann solver approximates the Riemann problem solution by two waves, one with the smallest and the other with the largest wave speed, respectively. This solution is then incorporated with upwind Godunov methods to solve the model equations as will be explained in Section 3. Further, we present the Godunov first-order upwind scheme based upon the HLL Riemann solver to solve the proposed model. To illustrate the performance of the HLL Riemann solver, we also implement it in the framework of the MUSCL-Hancock scheme [38].

This paper is organized as follows. Section 2 provides a brief resume of the model developed in [46]. The upwind Godunov methods for the principal part of the model are detailed in Section 3. Surprisingly, the extension of these methods to the model equations is simple and straightforward. In Section 4 we present some representative results from the numerical test cases that we conducted in the course of our study. The upwind Godunov methods are compared with unstaggered central schemes suggested in [35] in Section 4 as well. Finally, conclusions are drawn in Section 5.

2 Thermodynamically compatible two-phase flow model

We consider a thermodynamically compatible two-phase flow model originally presented in [25, 46] for porous material. The model describes the behaviour of a two-phase gas-solid mixture. It is assumed that the two phases are compressible and have their own mechanical properties. The model consists of balance laws for mass, momentum and energy in terms of parameters of state for the mixture along with additional closure governing equations. This paper focuses precisely on the development of numerical methods to solve the model equations, using upwind Godunov methods. The one-dimensional

conservation laws governing the model then are presented as follows [46]:

- Mixture mass conservation equation

$$\frac{\partial(\rho)}{\partial t}+\frac{\partial(\rho u)}{\partial x}=0. \tag{2.1}$$

- Mixture momentum conservation equation

$$\frac{\partial(\rho u)}{\partial t}+\frac{\partial(\rho u^2+P)}{\partial x}=0. \tag{2.2}$$

- Mixture energy conservation equation

$$\frac{\partial(\rho E)}{\partial t}+\frac{\partial(\rho uE+Pu)}{\partial x}=0. \tag{2.3}$$

The variables ρ, u, E and P represent, respectively, the density, velocity, energy and pressure for the mixture, t and x denote the time and the flow direction. The density and momentum are given by

$$\rho=\alpha\rho_1+(1-\alpha)\rho_2 \quad \text{and} \quad \rho u=\alpha\rho_1 u_1+(1-\alpha)\rho_2 u_2, \tag{2.4}$$

where the one, 1, and two, 2, are subscripts denotes the gas and solid phases, respectively, and $\alpha=\alpha_1$ is the volume concentration for the gas phase. It should be noted that the above mixture equations allow interphase exchange processes through additional conservation laws for the gas phase. Moreover, following the previous work [46], several closure laws must be given which involve the gas volume concentration balance law, mass gas concentration balance law and gas entropy concentration balance law.

- The gas volume concentration balance law

$$\frac{\partial(\rho\alpha)}{\partial t}+\frac{\partial(\rho u\alpha)}{\partial x}=\phi. \tag{2.5}$$

- The mass gas concentration balance law

$$\frac{\partial(\rho c)}{\partial t}+\frac{\partial(\rho uc)}{\partial x}=\psi. \tag{2.6}$$

- The gas entropy concentration balance law

$$\frac{\partial(\rho\chi)}{\partial t}+\frac{\partial(\rho u\chi)}{\partial x}=\omega, \tag{2.7}$$

where $c=c_1$ and $\chi=\chi_1$ are the mass concentration and entropy concentration for the gas phase. The terms on the right-hand side of (2.5)-(2.7) model the interphase exchange processes. The source term of (2.5) describes the relaxation of phase pressures to common uniform state with relaxation time $\tau^{(P)}$. This term has the form

$$\phi=\frac{-\rho}{\tau^{(P)}}\frac{\partial e}{\partial \alpha}. \tag{2.8}$$

The mass exchange ψ in (2.6) involves the rate of phase transition $\tau^{(c)}$ and is given by

$$\psi=\frac{-\rho}{\tau^{(c)}}\frac{\partial e}{\partial c}. \tag{2.9}$$

Finally, the energy exchange between the phases is taken to be

$$\omega=\frac{-\rho}{s\ \tau^{(\chi)}}\frac{\partial e}{\partial \chi}, \tag{2.10}$$

where $\tau^{(\chi)}$ is the rate of phase temperature coefficient.

To close system (2.1)-(2.3) and (2.5)-(2.7) we define the pressure and temperature for the mixture as

$$P=\rho^2\frac{\partial e}{\partial \rho}=\alpha_1\rho_1^2\frac{\partial e_1}{\partial \rho_1}+\alpha_2\rho_2^2\frac{\partial e_2}{\partial \rho_2}=\alpha P_1+(1-\alpha)P_2, \tag{2.11a}$$

$$T=\frac{\partial e}{\partial s}=\chi_1\frac{\partial e_1}{\partial s_1}+\chi_2\frac{\partial e_2}{\partial s_2}=\chi T_1+(1-\chi)T_2, \tag{2.11b}$$

with the volume concentrations and phase specific entropies are related by

$$\alpha_1+\alpha_2=1 \quad \text{and} \quad s=cs_1+(1-c)s_2. \tag{2.12}$$

Furthermore, the model equations (2.1)-(2.3) and (2.5)-(2.7) are supplemented by an equation of states for the mixture using the known equations of state of the constituents by the formulas

$$e=ce_1+(1-c)e_2 \quad \text{with} \quad E=e+\frac{u^2}{2}, \tag{2.13}$$

where e is the specific internal energy.

Eqs. (2.1)-(2.3) and (2.5)-(2.7) govern the two-phase gas-solid mixture problem. It is clear that these equations have at least six unknowns, namely ρ, u, E, α, c, χ for the mixture and phases, respectively. On the other hand, it is noted that these equations involve only conservative terms. Therefore, Eqs. (2.1)-(2.3) and (2.5)-(2.7) form a system of mixture conservation laws having a hyperbolic nature as discussed in the earlier investigation produced by the present author [46]. The eigenvalues of the system are

$$\lambda_1=u-a_m, \quad \lambda_{2,3,4,5}=u \quad \text{and} \quad \lambda_6=u+a_m, \tag{2.14}$$

where a_m is the speed of sound in the mixture [46]. It should also be noted that the system is not strictly hyperbolic because of the repeated second eigenvalue. Further, the characteristics for the mixture given by λ_1 and λ_6, respectively, are genuinely non-linear, while the characteristics given by $\lambda_{2,3,4,5}$ are linearly degenerate as shown in [46].

With the novel features of the governing equations system identified, this mathematical model is applicable to the wave dominant two-phase flow problems based on the Riemann problem. Further, it allows the application of modern numerical methods [33] which make use of the hyperbolic conservative nature of the flow equations.

3 Computational methods

In the present section, we will introduce upwind Godunov methods for solving the model equations. The conservation laws (2.1)-(2.3) and (2.5)-(2.7) governing the model can be written in the form

$$\frac{\partial \mathbb{U}}{\partial t}+\frac{\partial \mathbb{F}(\mathbb{U})}{\partial x}=\mathbb{S}(\mathbb{U}),\quad \forall x\in\mathbb{R},\quad t\in\mathbb{R}^+, \tag{3.1}$$

where

$$\mathbb{U}=\begin{pmatrix}\rho\\ \rho\alpha\\ \rho u\\ \rho c\\ \rho\chi\\ \rho E\end{pmatrix},\quad \mathbb{F}(\mathbb{U})=\begin{pmatrix}\rho u\\ \rho u\alpha\\ \rho u^2+P\\ \rho uc\\ \rho u\chi\\ \rho uE+Pu\end{pmatrix}\quad \text{and}\quad \mathbb{S}(\mathbb{U})=\begin{pmatrix}0\\ \phi\\ 0\\ \psi\\ \omega\\ 0\end{pmatrix}. \tag{3.2}$$

The numerical approach employed in this paper for the solution of the above system is based on the methodology of upwind Godunov methods for general systems of hyperbolic conservation laws. Upwind Godunov methods require the solution of the Riemann problem which may be an exact solution or an approximate solution. For the present model the exact solution of the Riemann problem is complicated and not known in a closed form. Indeed, the explicit formulas in the Riemann invariants are not possible for complex equations of state for the solid and gas phases. Thus, approximate Riemann solvers are considered. Among the available approximate Riemann solvers is the HLL Riemann solver [9,33] which is a direct approximation of the upwind flux computations. For the current two-phase gas-solid mixture, the approximate solution to the Riemann problem for the model equations is based on the HLL Riemann solver. This solution is then employed in the construction of the Godunov first-order upwind scheme and in the MUSCL-Hancock scheme to solve the general initial-boundary value problem for the two-phase gas-solid mixture. In this paper we are mainly interested in the principal part of Eq. (3.1) in processes without dissipation, that is we set $\mathbb{S}(\mathbb{U})=0$. More information concerning the source terms effects can be found in the recent paper [46], which is beyond the scope of this paper.

A conservative description of (3.1) in processes without dissipation over a time step Δt over a cell I_i yields

$$\mathbb{U}_i^{n+1}=\mathbb{U}_i^n-\frac{\Delta t}{\Delta x}\left[\mathbb{F}_{i+\frac{1}{2}}-\mathbb{F}_{i-\frac{1}{2}}\right]. \tag{3.3}$$

In (3.3) Δx is cell spacing and Δt is the time step determined by

$$\Delta t=\text{CFL}\cdot\frac{\Delta x}{S_{\max}}, \tag{3.4}$$

for which $0<\text{CFL}\leq 1$ is the Courant number coefficient CFL and $S_{\max}$ is the maximum wave speed at the current time level n chosen as

$$S_{\max}=\max_i\{|\lambda_i|\}, \tag{3.5}$$

where λ_i are the eigenvalues corresponding to sound waves. $\mathbb{F}_{i+1/2}$ is the upwind numerical flux computed at the interface $x_{i+1/2}$ by solving the initial-boundary value problem for the two-phase gas-solid mixture defined by (3.1), for $\mathbb{S}(\mathbb{U})=0$, over the time interval $\Delta t=t^{n+1}-t^n$ together with the initial conditions

$$\mathbb{U}(x,t^n)=\begin{cases}\mathbb{U}_L, & \text{for } x<x_{i+\frac{1}{2}},\\ \mathbb{U}_R, & \text{for } x>x_{i+\frac{1}{2}},\end{cases} \tag{3.6}$$

where $\mathbb{U}_L$ and $\mathbb{U}_R$ are given left and right constant states of the two-phase gas-solid mixture. This is known as the Riemann problem. Fig. 1 shows the structure of the Riemann problem for the model equations. The three waves divide the $x-t$ plane into four regions corresponding to the four states $\mathbb{U}_L$, $\mathbb{U}_L^*$, $\mathbb{U}_R^*$ and $\mathbb{U}_R$ as shown in Fig. 1. The two nonlinear waves $\lambda_1=\lambda_L$ and $\lambda_6=\lambda_R$ represent either shocks or rarefactions separated by a middle wave λ_m of multiplicity four moving at the phase velocity.

The numerical procedure introduced in the following sections is for calculating the numerical flux $\mathbb{F}_{i+1/2}$. It is, however, enough to employ one approximate Riemann solver to have a numerical flux.

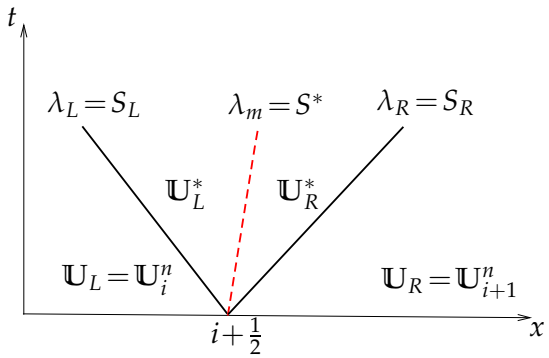

Figure 1: Graphical representation of the Riemann problem in the $x-t$ plane with initial states $\mathbb{U}_L$ and $\mathbb{U}_R$. These data decompose into two non-linear waves with speeds S_L and S_R and a linear wave with velocity S^*. The three waves divide the $x-t$ plane into four regions each defining a constant state: $\mathbb{U}_L$, $\mathbb{U}_L^*$, $\mathbb{U}_R^*$ and $\mathbb{U}_R$. The outermost states, $\mathbb{U}_L$ and $\mathbb{U}_R$, are given as input to the problem, while the remaining ones have to be determined.

3.1 HLL Riemann solver

In this paper we employ the HLL Riemann solver [9] which is a direct approximation of the numerical flux to compute the upwind Godunov flux. The HLL Riemann solver consists of two waves with three constant states. It is also very efficient and robust, and provides a physical and entropy satisfying solution. Due to the mathematical nature of the model equations, the HLL Riemann solver is applied directly to the system describing two-phase gas-solid mixture without any modification with the following HLL flux [9,33]

$$\mathbb{F}^{\text{HLL}}_{i+\frac{1}{2}}=\begin{cases}\mathbb{F}_L, & 0\le S_L,\\ \mathbb{F}^*_L=\mathbb{F}_L+S_L\big(\mathbb{U}^{\text{HLL}}-\mathbb{U}_L\big), & S_L\le 0\le S^*,\\ \mathbb{F}^*_R=\mathbb{F}_R+S_R\big(\mathbb{U}^{\text{HLL}}-\mathbb{U}_R\big), & S^*\le 0\le S_R,\\ \mathbb{F}_R, & 0\ge S_R.\end{cases} \tag{3.7}$$

The notations, S_L and S_R are referred to as the speeds of the smallest and largest waves assumed to be known. While the vector $\mathbb{U}^{\text{HLL}}$ is the constant state vector given by

$$\mathbb{U}^{\text{HLL}}=\frac{S_R\mathbb{U}_R-\mathbb{F}_R-S_L\mathbb{U}_L+\mathbb{F}_L}{S_R-S_L}, \tag{3.8}$$

which is the average of the exact Riemann problem between the slowest and fastest waves [33].

Since the HLL Riemann solver assumes two waves system, it follows that $\mathbb{F}^*_L$ and $\mathbb{F}^*_R$ are the same as the HLL flux, $\mathbb{F}^{\text{HLL}}_{i+1/2}$, is then given by

$$\mathbb{F}^{\text{HLL}}_{i+\frac{1}{2}}=\frac{S_R\mathbb{F}_L-S_L\mathbb{F}_R+S_R(\mathbb{U}_R-\mathbb{U}_L)S_L}{S_R-S_L}. \tag{3.9}$$

The HLL Riemann solver requires the estimates of wave speeds S_L and S_R in the Riemann problem. A direct and simple wave speed estimates follow from the eigenvalues of the model equations, given analytically by (2.14)

$$S_L=u_L-a_{mL}\quad\text{and}\quad S_R=u_R+a_{mR}, \tag{3.10}$$

is quite sufficient for the purposes here. An extensive and detailed review of all possible estimates for these velocities can be found in [33]. In the next sections we will make use of the HLL flux when constructing upwind Godunov methods.

3.2 The Godunov first-order upwind scheme

The Godunov scheme is to find the solution of the Riemann problem for the two-phase gas-solid mixture. This scheme is a first-order accurate scheme which can be written in the conservative form (3.3) with interface flux given by

$$\mathbb{F}_{i+\frac{1}{2}}=\mathbb{F}\big(\mathbb{U}_{i+\frac{1}{2}}(0)\big), \tag{3.11}$$

where $\mathbb{U}_{i+1/2}(0)$, estimated at $x/t=0$, is the local Riemann problem solution at the cell interface position $i+1/2$ of the mixture conservation laws (3.3) with the following initial conditions

$$\mathbb{U}(x,0)=\begin{cases}\mathbb{U}_L, & \text{for } x<x_0,\\ \mathbb{U}_R, & \text{for } x>x_0,\end{cases} \tag{3.12}$$

where x_0 represent the initial discontinuity. The solution of the Riemann problem for the current model equations can be exact, analytical, or approximate. However, as the authors pointed out that the development of an analytical solution to the Riemann problem for the current model is not available at this time. This is due to the complex nature of the model equations and it is not easy to iterate each wave for the mixture and the phases separately. Thus, the solution of the Riemann problem is determined using the HLL Riemann solver (3.9), which we have described in the previous section and now considered to be the approximate solutions for the upwind numerical fluxes given by (3.3).

3.3 The MUSCL-Hancock scheme

Apart from flux calculation, the Godunov first-order upwind scheme can be extended to second-order accuracy following the MUSCL-Hancock approach [38]. The MUSCL-Hancock approach is based on the following three steps [33].

- Data reconstruction. In this step the cell averaged values $\mathbb{U}_i^n$ are locally restored by piecewise linear function in every cell I_i

$$\mathbb{U}_i(x)=\mathbb{U}_i^n(x)+\frac{(x-x_i)}{\Delta x}\Delta_i. \tag{3.13}$$

  This step consists of changing $\mathbb{U}_i$ values as

$$\mathbb{U}_i^L=\mathbb{U}_i^n-\frac{\Delta_i}{2} \quad \text{and} \quad \mathbb{U}_i^R=\mathbb{U}_i^n+\frac{\Delta_i}{2}, \tag{3.14}$$

  which is known as the boundary extrapolated values. In the above expressions Δ_i is a limited slope vector of six components for the current two-phase gas-solid mixture which can be written as

$$\Delta_i=\frac{1}{2}\Big((1+\omega)\Delta_{i-\frac{1}{2}}+(1-\omega)\Delta_{i+\frac{1}{2}}\Big),$$

  where

$$\Delta_{i-\frac{1}{2}}=\mathbb{U}_i^n-\mathbb{U}_{i-1}^n, \quad \Delta_{i+\frac{1}{2}}=\mathbb{U}_{i+1}^n-\mathbb{U}_i^n \quad \text{and} \quad \omega\in[-1,1].$$

  Furthermore, this limiter is used to avoid spurious oscillations near large gradients of the numerical solution and obtained using the TVD constraints as follows

$$\Delta_i=\begin{cases}\max\Big[0,\min(\Lambda\,\Delta_{i-\frac{1}{2}},\Delta_{i+\frac{1}{2}}),\min(\Delta_{i-\frac{1}{2}},\Lambda\Delta_{i+\frac{1}{2}})\Big], & \Delta_{i+\frac{1}{2}}>0,\\ \min\Big[0,\max(\Lambda\,\Delta_{i-\frac{1}{2}},\Delta_{i+\frac{1}{2}}),\max(\Delta_{i-\frac{1}{2}},\Lambda\Delta_{i+\frac{1}{2}})\Big], & \Delta_{i+\frac{1}{2}}<0,\end{cases} \tag{3.15}$$

where the parameter Λ represent a particular limiter of interest. See [33] for several choices for the slope limiter and [43] for two-phase flow applications.

- Evolution. The boundary extrapolated values $\mathbb{U}_i^L$ and $\mathbb{U}_i^R$ in (3.14) are evolved by half a time step for every cell I_i. They are calculated as

$$(\mathbb{U}_i^L)^{\text{New}} = \mathbb{U}_i^L + \frac{1}{2}\frac{\Delta t}{\Delta x}\big[\mathbb{F}(\mathbb{U}_i^L) - \mathbb{F}(\mathbb{U}_i^R)\big], \tag{3.16a}$$

$$(\mathbb{U}_i^R)^{\text{New}} = \mathbb{U}_i^R + \frac{1}{2}\frac{\Delta t}{\Delta x}\big[\mathbb{F}(\mathbb{U}_i^L) - \mathbb{F}(\mathbb{U}_i^R)\big], \tag{3.16b}$$

  where the intercell fluxes are calculated at the boundary extrapolated values of each cell. Note that this step is just an intermediate step with two different fluxes, $\mathbb{F}(\mathbb{U}_{i+1}^L)$ and $\mathbb{F}(\mathbb{U}_i^R)$, at each intercell position $i+1/2$. Still, the intercell flux $\mathbb{F}_{i+1/2}$ appearing in (3.3) needs to be computed.

- The Riemann problem. The interface flux, $\mathbb{F}_{i+1/2}$, is calculated by solving the conventional Riemann problems with the evolved data $(\mathbb{U}_{i+1}^L)^{\text{New}}$ and $(\mathbb{U}_i^R)^{\text{New}}$ as follows

$$\mathbb{F}_{i+\frac{1}{2}} = \mathbb{F}_{i+\frac{1}{2}}\Big(\big(\mathbb{U}_i^R\big)^{\text{New}}, \big(\mathbb{U}_{i+1}^L\big)^{\text{New}}\Big). \tag{3.17}$$

  In the above expression, the HLL Riemann solver is employed as described in Section 3.1. The solution then is advanced by Δt from t^n using the explicit formula (3.3).

4 Numerical results

The primary focus of this paper is to explore upwind Godunov methods, gain from their experience and efforts on the thermodynamically compatible two-phase flow model presented in the current paper, rather than developing new numerical methods to solve such a model. Thus, to illustrate the performance of the proposed upwind Godunov methods and show the advantages of the present mathematical model for the two-phase gas-solid mixture, a series of numerical test cases are considered. These test cases were taken from [33, 34, 45, 46]. The first test case includes a sonic rarefaction wave within two-phase gas-solid mixture. In the second test case we consider a two rarefaction waves and a non-trivial contact discontinuity. In the third test case, we consider a collision of two-phase gas-solid mixture which consists of a symmetric Riemann problem. Finally, the fourth test case deals with the propagation of a volume concentration wave within a two-phase gas-solid mixture. For all test cases we make use of the HLL Riemann solver of Section 3.1 within two numerical methods, namely the Godunov first-order upwind scheme and the MUSCL-Hancock scheme. As will be seen from the solutions presented in later sections, the initial conditions of these test cases, given in Tables 1 and 2, consists of two constant left and right states separated by a contact discontinuity at a position

Table 1: Initial states for numerical test 4.1.

Left	Right
$\alpha_L=0.7$	$\alpha_R=0.2$
$\rho_{1L}=1.0$	$\rho_{1R}=0.125$
$u_{1L}=250.0$	$u_{1R}=0.0$
$\rho_{2L}=1.0$	$\rho_{2R}=0.125$
$u_{2L}=250.0$	$u_{2R}=0.0$

Table 2: Left and right initial states for the two-phase gas-solid mixture Riemann problem for numerical tests 4.2-4.4.

Test case	α_L	ρ_L	u_L	χ_L	s_L	α_R	ρ_R	u_R	χ_R	s_R
2	0.95	70.0	-100.0	0.0	0.0	0.05	70.0	100.0	0.0	0.0
3	0.1	0.1	800.0	0.0	0.0	0.1	0.1	-800.0	0.0	0.0
4	0.0	100.0	0.0	0.0	0.0	1.0	50.0	0.0	0.0	0.0

$x=x_0$ at time $t=0$. In addition, all the results are displayed with the relevant gas mass concentration being calculated by

$$c=\frac{\alpha\rho_1}{\rho}.$$

The equations of state (EOS) for the two-phase gas-solid mixture is given by (2.13) and determined by the equations of state for the solid and gas phases. For the purposes of this paper, the solid phase is governed by the Mie-Grüneisen equation of state [46]

$$e_2=\frac{A_1^2}{2A_2^2}\Big[\Big(\frac{\rho}{\rho_2^0}\Big)^{A_2}-1\Big]^2+c_v^2A_3\Big(\frac{\rho}{\rho_2^0}\Big)^{A_4}\Big[\exp\Big(\frac{s}{c_v^2}\Big)-1\Big]-\frac{A_5}{\rho}, \tag{4.1}$$

with the relevant constants: $\rho_2^0=2.77$, $c_v^2=0.00045$, $A_1=6$, $A_2=1.08$, $A_3=293$, $A_4=2.11$ and $A_5=0.1$. For the gas phase, we use the perfect gas EOS as [46]

$$e_1=\frac{A_0}{\rho_1^0(\gamma-1)}\Big(\frac{\rho}{\rho_1^0}\Big)^{\gamma-1}\exp\Big(\frac{s}{c_v^1}\Big), \tag{4.2}$$

where the parameters are taken as γ=1.4, ρ_1^0=1, c_v^1=720 and A_0=1×10^5, if not mentioned otherwise, being employed throughout.

The above equations of state are involved in all computations. It should be noted that the Mie-Grüneisen EOS is more complex type EOS than the perfect gas EOS. Further, due to the complexity of the solid phase EOS, no exact solution is available to the model equations as mentioned earlier. However, it is possible to compute oscillation-free solutions using the Mie-Grüneisen EOS with the proposed upwind Godunov methods. That is, the solutions are evaluated by means of reducing the spurious (non-physical) oscillations observed at discontinuities by upwind Godunov methods based on an approximate Riemann solver. For reference solution purposes then, the numerical results on a very fine

mesh offers a guideline to the wave structure in every test case. This reference solution is taken from the TVD MUSCL-Hancock computations using the HLL Riemann solver with 4000 mesh cells, as meshes of a larger number of cells were checked to produce no further improvement. We have chosen to use the MUSCL-Hancock scheme together with the SUPERBEE limiter as a reference solution since it has a unique success in many practical computations, see for example [16]. In addition, the present results have considerable better accuracy than previous results, see [46]. All the numerical solutions are performed on a domain of 100m long with transmissive boundary conditions being used. The Courant number coefficient is CFL$=0.9$. For each test, we use SUPERBEE limiter for the MUSCL-Hancock scheme to control spurious oscillations associated in the vicinity of strong gradients. Further, to demonstrate the advantage of the present TVD MUSCL-Hancock, the results are compared with the reference solution of [46], whose numerical accuracy was confirmed using the SLIC scheme together with the SUPERBEE limiter. In all computations, we examine the numerical solutions on a coarse mesh of 100 cells at a given time of interest using the TVD MUSCL-Hancock and Godunov first-order methods. The results are also compared with the Lax-Friedrichs scheme which is an independent and iteration-free scheme.

In order to further validate the model equations and the numerical methods employed in the current paper, we compare the present simulation results with an alternative numerical method available in the literature. As mentioned earlier, there exist a variety of numerical methods for solving hyperbolic conservation laws that arise in many physical problems. One such method is the unstaggered central scheme of [35] which is a relatively modern finite volume numerical method for solving hyperbolic conservation laws. We shall refer to the unstaggered central scheme as UCS. The UCS technique is an extension of the standard Nessyahu and Tadmor central scheme [20] that does not require two staggered grids. Furthermore, it evolves the numerical solution on a unique grid and avoids the resolution of the associated Riemann problems at the cell interfaces. That is, the UCS is classified as a non-oscillatory second-order accurate Riemann-free solvers numerical method that can be written in the form (3.3). Recently, the UCS approach has been prototyped in its preliminary version to solve the shallow water equations [35], for which we refer the reader for further details. To solve the principal part of the model equations then, the UCS procedure uses two steps to implement. The first step employs ghost staggered cells to estimate the solution at the new time step within these cells as follows [35]

$$\mathbb{U}^{\mathrm{G}}{}_{i+\frac{1}{2}}=\frac{1}{2}(\mathbb{U}^{n}_{i+1}+\mathbb{U}^{n}_{i})+\frac{1}{8}\Big((\mathbb{U}^{n}_{i})'-(\mathbb{U}^{n}_{i+1})'\Big)-\frac{\Delta t}{\Delta x}\Big(\mathbb{F}(\mathbb{U}^{n+\frac{1}{2}}_{i+1})-\mathbb{F}(\mathbb{U}^{n+\frac{1}{2}}_{i})\Big), \tag{4.3}$$

where $\mathrm{G}_{i+1/2}=[x_i,x_{i+1}]$ is the ghost staggered cells and $(\mathbb{U}^{n}_{i})'$ denotes the slope approximation to first-order accuracy. This solution then is taken back to the original grid using the following formula

$$\mathbb{U}^{n+1}_{i}=\frac{1}{2}\Big(\mathbb{U}^{G}_{i-\frac{1}{2}}+\mathbb{U}^{G}_{i+\frac{1}{2}}\Big)+\frac{1}{8}\Big((\mathbb{U}^{G}_{i-\frac{1}{2}})'-(\mathbb{U}^{G}_{i+\frac{1}{2}})'\Big), \tag{4.4}$$

which is regarded as the final solution. In what follows, the symbols in each plot correspond to the numerical solutions using the four different numerical methods while the reference solutions are given by the solid lines in each plot. Finally, the reader is referred to the web version of this paper for interpretation of the waves to colour in all the figures legend throughout.

4.1 Sonic rarefaction wave within gas-solid mixture

To demonstrate the advantages of the present mathematical model and numerical methods, the sonic rarefaction test case [33] for single-phase flow is tested. This test case was also extended to two-phase flow in [34]. In [34], two phases and two different types of EOS in the simplest form are tested for a two-fluid model type of two-phase flow. In this paper we extended the sonic rarefaction test case to the mathematical model adopted in this paper with a different type of EOS for both the solid phase and the gas phase. In addition, the interest of this test case lies in assessing the entropy satisfaction property of the numerical methods. For this test case, it is known [33,34] that the wave structure consists of a left sonic rarefaction wave, a right travelling contact discontinuity and a right

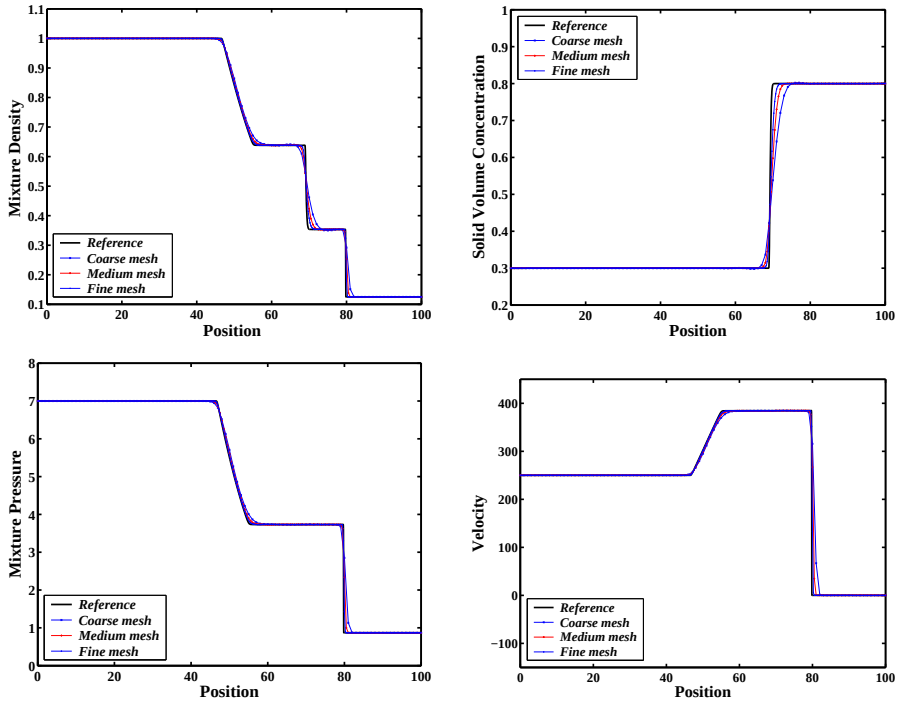

Figure 2: Sonic rarefaction wave test case at time $t=0.01$. Computations are carried out under different mesh resolutions for the MUSCL-Hancock scheme together with the SUPERBEE limiter using the HLL Riemann solver. Top panel: mixture density (kg m^{-3}) and solid volume concentration. Bottom panel: mixture pressure (Pa) and velocity (m s^{-1}). The solid lines give the reference solutions by the TVD SLIC scheme of [46] for two-phase gas-solid mixture, 4000 mesh cells are used in the computations at time $t=0.01$.

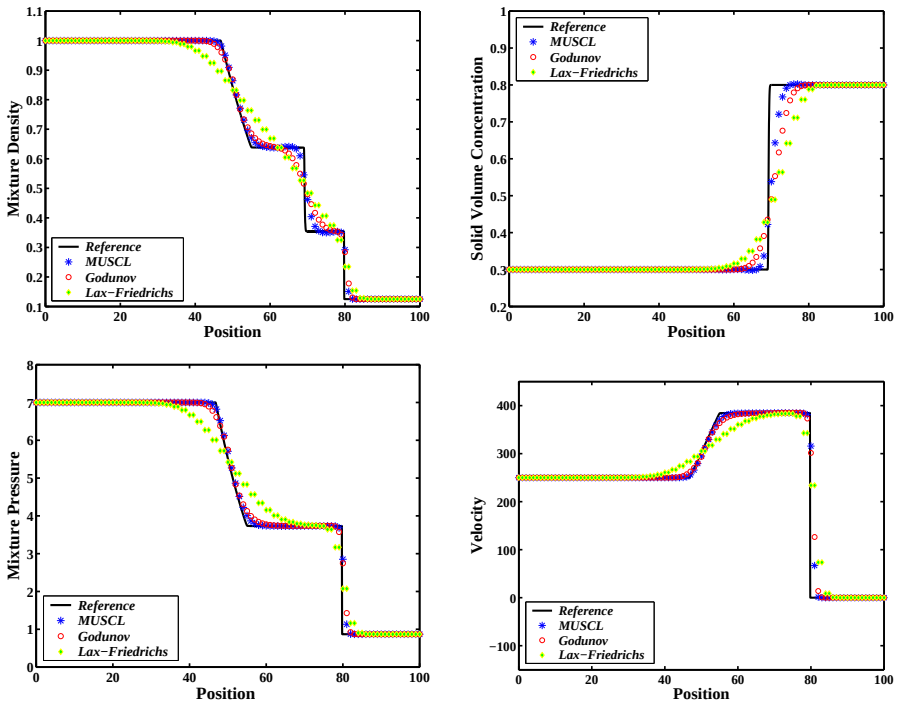

Figure 3: Solution of the sonic rarefaction wave (test case 4.1) computed with three numerical methods at time $t=0.01$ on 100 mesh cells with the SUPERBEE limiter. From left to right and top to bottom: mixture density (kg m^{-3}), solid volume concentration, mixture pressure (Pa) and velocity (m s^{-1}). The solid lines give the reference solution as computed from [46] of two-phase gas-solid mixture. The results are similar to previous ones proposed in the literature for two-phase flows.

shock wave. The initial conditions are given in Table 1. These initial conditions are such that as the time progresses, the two-phase gas-solid mixture generate a left sonic rarefaction wave and a right shock wave, for the mixture, separated by a right travelling contact discontinuity as shown in Fig. 2. Fig. 2 gives numerical results (symbols) of the mixture density, solid volume concentration, mixture pressure and velocity at time $t=0.01$ using three different meshes, 100, 200 and 400 cells. From Fig. 2, the mesh convergence to the reference solution (given by solid lines) of [46] can be seen in all the plots. The good agreement of the solution behaviour with the reference solution is also seen. As regard to the reference solution, the reference solutions are provided using the TVD SLIC scheme of [46] which is prepared separately on a very fine mesh of 4000 cells.

Fig. 3 compares the performance of the Godunov first-order upwind scheme and the TVD MUSCL-Hancock scheme using the HLL Riemann solver at time $t=0.01$ using 100 mesh cells. From the figure, it is easy to observe the agreement between the numerical (symbols) and reference solutions (solid lines) for the three methods. The reference solutions in Fig. 3 are provided by the MUSCL-Hancock scheme together with the HLL Riemann solver using the SUPERBEE limiter on a mesh of 4000 cells. Furthermore, the presented results are very similar to those obtained in [34]. It is clear that the results

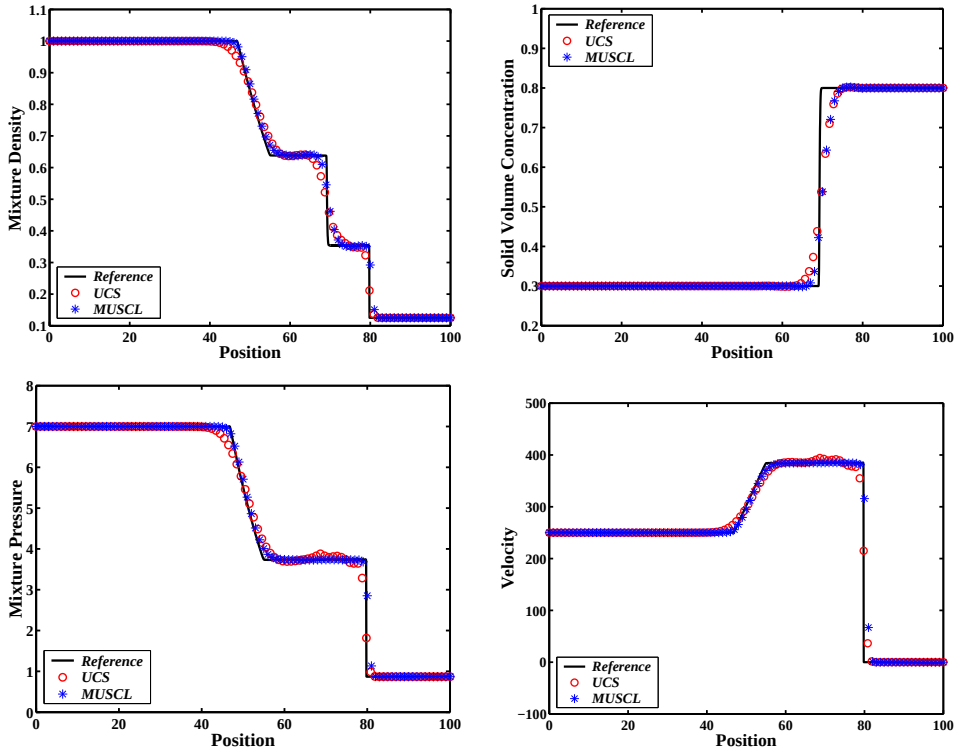

Figure 4: Comparison of computed results, shown with symbols, for test case 4.1 with the reference solution which is provided by the TVD MUSCL-Hancock scheme based on the HLL Riemann solver. The UCS approach of [35] is used to solve the model equations in processes without dissipation at time $t=0.01$ on 100 mesh cells with 0.485 CFL coefficient. As in Figs. 2 and 3, from left to right and top to bottom, mixture density (kg m^{-3}), solid volume concentration, mixture pressure (Pa) and velocity (m s^{-1}). The obtained results validate the model equations and illustrate robustness and performance of the numerical methods.

provided by the TVD MUSCL-Hancock scheme are oscillation-free and attain sharper representation of the contact discontinuity when compared to the Godunov first-order upwind and Lax-Friedrichs methods. In addition, it is easily observed from Fig. 3 that the correct resolution of the sonic point satisfying the entropy property of the proposed numerical methods.

To further validate the proposed numerical solutions computed using upwind Godunov methods, we solve the model equations using the unstaggered central scheme, UCS, of [35] which is a Riemann-free solver. Fig. 4 shows a comparison of the numerical resolution given by the UCS and the numerical results of the TVD MUSCL-Hancock scheme using the HLL Riemann solver at time $t=0.01$ using 100 mesh cells. The latter is in excellent agreement with the UCS resolutions, and both methods are in a very good agreement with the reference solution. Note that the spurious oscillations generated by the UCS across the contact discontinuity are due the non-linearity of the model equations.

In conclusion, the numerical results reported in this section compare well with the reference solution and validate both model equations and the numerical methods.

4.2 Rarefaction waves propagation within gas-solid mixture

This test case has been previously studied in [46] with Godunov methods of centred-type. The solution for this test case is composed of a left rarefaction wave and a right rarefaction wave separated by a non-trivial contact discontinuity as presented in Fig. 5. In this figure the results (symbols) on a mesh of 100 cells using the TVD MUSCL-Hancock, the first-order Godunov and Lax-Friedrichs methods are displayed and compared with the reference solutions (solid lines).

As regard to the reference solution, the TVD MUSCL-Hancock scheme with the HLL Riemann solver provides an accurate and consistent results on a very fine mesh of 4000 cells. The three methods are in excellent agreement with the reference solutions. In Fig. 5, we note a jump in the mixture density and the solid temperature across the non-trivial contact discontinuity. This is caused by the existence of two separate volume concentration waves in the gas phase, see Table 2. It is also clear that across the middle wave both the first-order Godunov and Lax-Friedrichs methods attain inferior representation of the contact discontinuity. Whereas the TVD MUSCL-Hancock scheme achieves a sharper

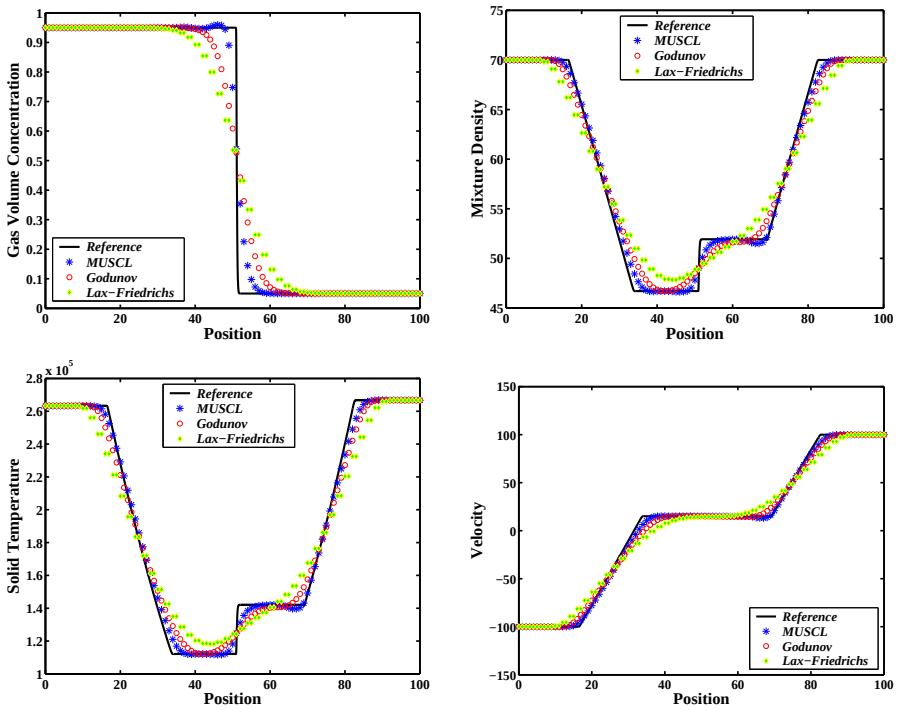

Figure 5: Present numerical solutions (symbols) from three numerical methods (TVD MUSCL-Hancock and Godunov first-order upwind, with the HLL Riemann solver, and Lax-Friedrichs) calculated on 100 mesh cells at time $t=0.015$, test case 4.2. Solid lines are used to identify results computed with the MUSCL-Hancock scheme together with the SUPERBEE limiter on 4000 mesh cells. The top left and right panels show the gas volume concentration and mixture density (kg m^{-3}), respectively. While in the bottom left and right panels show the solid temperature (K) and velocity (m s^{-1}), respectively. The major difference between the three methods is the resolution of the contact wave.

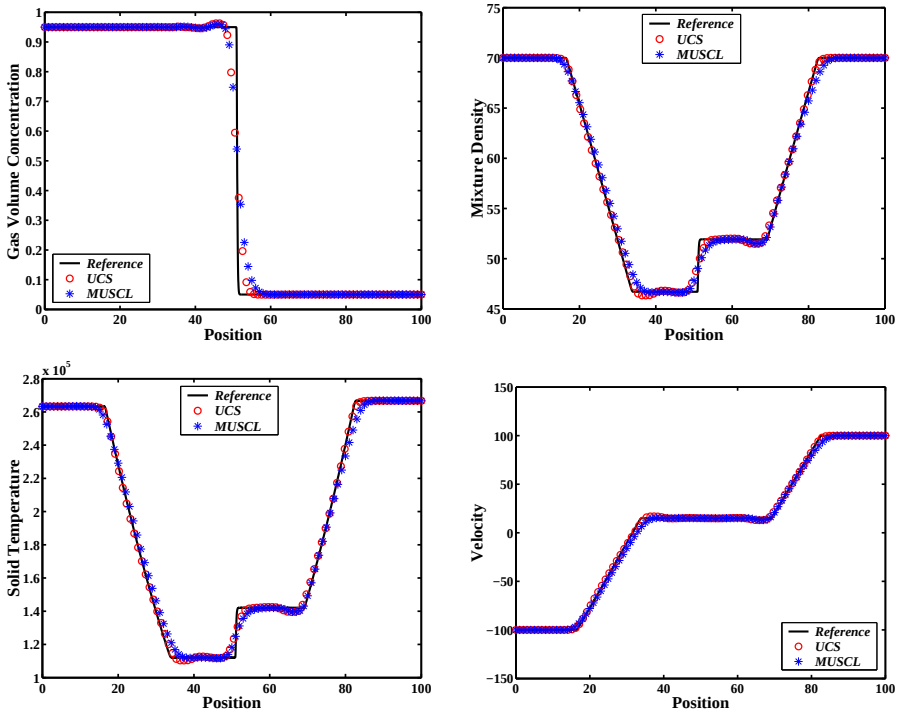

Figure 6: Numerical (symbols) and reference solutions (solid lines) of the rarefaction waves propagation within gas-solid mixture, test case 4.2. Comparison for the UCS and MUSCL-Hancock techniques at time $t=0.015$ for a 100 cell mesh. The UCS approach has been carried out with CFL $=0.485$. From left to right, the top panel shows the gas volume concentration and mixture density (kg m^{-3}), respectively, whereas in the bottom left and right panels show the solid temperature (K) and velocity (m s^{-1}), respectively.

representation of the contact discontinuity. On the other hand, clear advantages in the use of TVD MUSCL-Hancock scheme are evident in the resolution of the head and the tail of the rarefaction waves. Further, it is observed that the TVD MUSCL-Hancock scheme results are completely oscillation-free with the proposed mathematical model.

Profiles of the same flow variables are plotted at time $t=0.015$ in Fig. 6 for the sake of comparisons. Fig. 6 illustrates a comparison of the reference solution (solid lines) and the computed, numerical, resolutions (symbols) using TVD MUSCL-Hancock scheme of section 3.3 and the UCS of [35] with a mesh of 100 cells. Clearly, the numerical solutions compare very well with the reference solution. Also, the numerical results provided by the UCS around the non-trivial contact discontinuities exhibits some of the spurious oscillations. As an approximation, however, the non-trivial contact discontinuities resolutions follow closely the reference solutions.

To get more insight in the model equations, a solution to the full system is presented in Fig. 7. The computations are carried out with equal gas volume concentration, $\alpha_L=0.5=\alpha_R$. The solution, therefore, is composed of two symmetric rarefaction waves separated by a trivial contact discontinuity. Fig. 7 shows the solutions for the mixture pressure, mixture density, solid temperature and the velocity at time $t=0.015$.

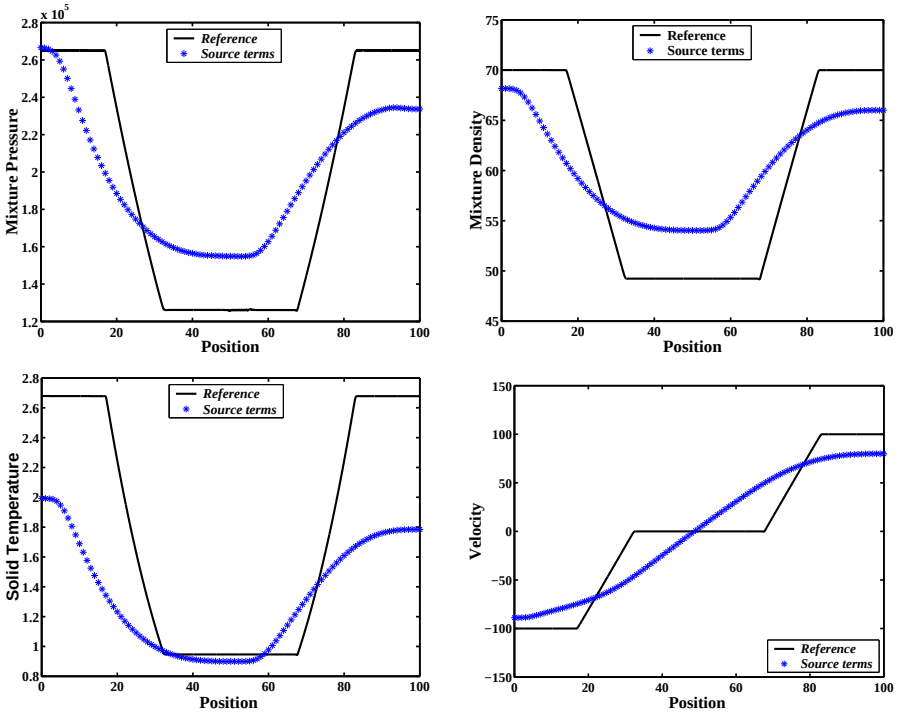

Figure 7: Numerical solutions (symbols) for the model system at time $t=0.015$ on 100 mesh cells with a gas volume concentration equal to 0.5 on the left and right given initial conditions of the Riemann problem. The solid black lines indicate the reference solution. Results shown for the mixture pressure (Pa, top left) and the mixture density (kg m^{-3}, top right), solid temperature (K, bottom left) and velocity (m s^{-1}, bottom right). The configuration is similar to that of Fig. 5, but the middle wave is a trivial contact discontinuity.

The symbol curves represent the source terms appearing in (2.8)-(2.10) whereas the solid line represent the reference solution of the model equations with no source terms. With the source terms involved in the gas volume concentration, mass gas concentration and gas entropy concentration, phase interaction is predicted to take place immediately and flow variables decreases as it passes through the wave structure. In other words, when the parameters $\tau^{(p)}$, $\tau^{(c)}$ and $\tau^{(\chi)}$ eventually becomes high enough, that is 100, the left and right propagating waves and the trivial contact discontinuities have a continuous structure all over the domain as displayed by the symbols, see Fig. 7. Furthermore, one can observe that there are discrepancies or particular behavior when solving the complete model equations in comparison to the reference solution. In particular, the solid temperature and the mixture density indicate visible discrepancy from the reference solution results. It is interesting to point out that when the CFL number is reduced to 0.1 the source terms inclusion shows such discrepancies, for which the authors observed the same behavior in [46]. In the current gas-solid two-phase mixture computations the differences within the source terms in the current model equations continues to deteriorate the accuracy of the current simulations. The source terms for the current model equations are an interesting problem which needs to be researched further in the future.

4.3 Gas-solid mixture collision

This test case is an extension of a collision test case in [46] for two-phase gas-solid mixture. The initial conditions are give in Table 2. These initial conditions produce two strong fast shock waves propagating symmetrically in opposite direction separated by a trivial contact discontinuity as shown in Fig. 8 at time $t=0.004$. In Fig. 8 results (symbols) for some flow profiles from three numerical methods, the MUSCL-Hancock, the first-order Godunov upwind and the Lax-Friedrichs, at time $t=0.004$ are displayed. All the solutions are compared with a reference solution (solid lines) computed using the TVD MUSCL-Hancock scheme with the HLL Riemann solver on a very fine mesh of 4000 cells. The plots in Fig. 8 show that the three methods provide a similar resolution of the wave structure as the reference solution. Fig. 8 also indicates that the three methods behave similar near the shock waves, but differ in their ability to resolve the contact discontinuity. For MUSCL-Hancock scheme, the solutions at the coarsest resolution are essentially oscillation-free for all the state profiles. Further, it can be observed that the MUSCL-Hancock scheme captures sharper waves than the first-order Godunov upwind scheme.

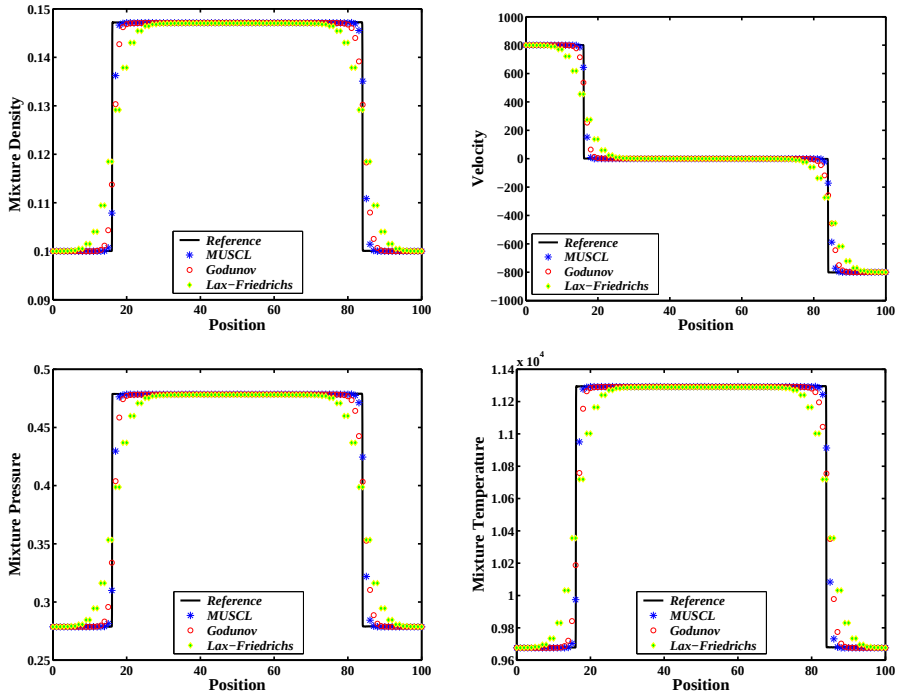

Figure 8: Results obtained for mixture density (kg m^{-3}) and velocity (m s^{-1}), mixture pressure (Pa) and mixture temperature (K) for gas-solid mixture collision (test case 4.3) using the TVD MUSCL-Hancock and Godunov first-order upwind, with the HLL Riemann solver, and Lax-Friedrichs methods. Computations (symbols) are carried out at time $t=0.004$ on 100 mesh cells. The reference solutions (solid lines) have been obtained by means of the TVD MUSCL-Hancock scheme with the HLL Riemann solver using 4000 mesh cells.

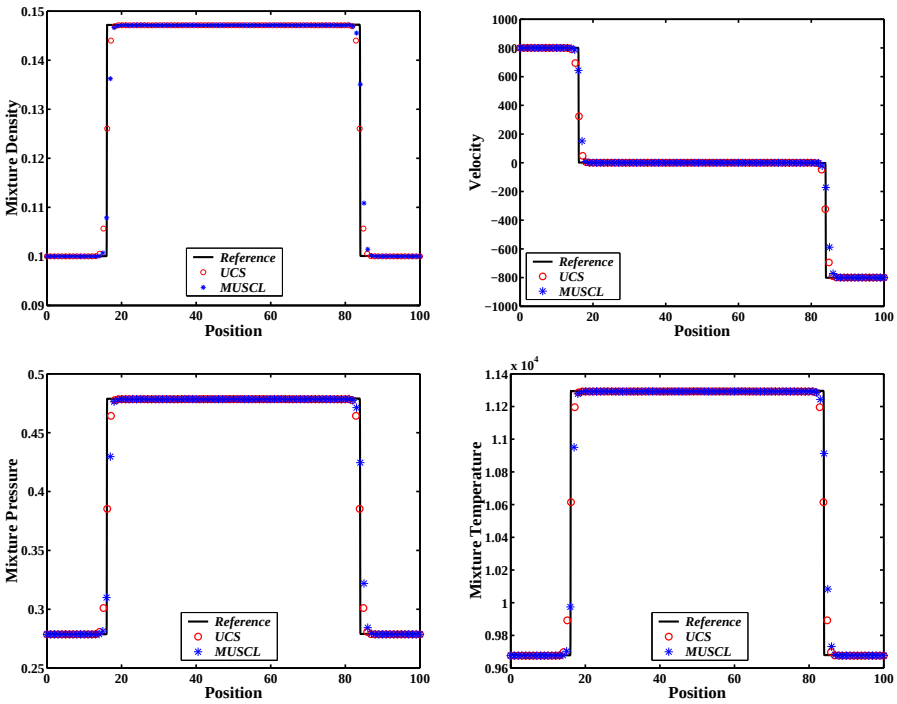

Figure 9: Comparison for the gas-solid mixture collision (test case 4.3) for the MUSCL-Hancock scheme with UCS approach for 100 mesh cells. The CFL of 0.485 has been used for the UCS approach. Numerical and reference solutions are given for the profiles of mixture density (kg m^{-3}), velocity (m s^{-1}), mixture pressure (Pa) and mixture temperature (K) at time t=0.004. An excellent agreement is observed throughout the profiles.

For this test case also, we display in Fig. 9 numerical results (symbols) using the UCS approach [35]. In Fig. 9 we illustrate a comparison between the TVD MUSCL-Hancock scheme and the UCS approach on a 100 mesh cells. From the comparisons, we find that both methods reproduce the same wave structure without any spurious oscillations at discontinuities throughout the computations. Once more, excellent agreement between the numerical resolutions and the reference solutions in the two-phase gas-solid mixture collision is clearly observed.

4.4 Propagation of a volume wave within a gas-solid mixture

This test case was presented in [46] for two-phase gas-solid mixture. The solution for the mixture consists of a left rarefaction wave and right shock wave separated by a contact discontinuity as displayed in Fig. 10. Fig. 10 shows the numerical results for some state profiles, namely the mixture density, velocity, mixture pressure and gas volume concentration at time $t=0.01$. These results (symbols) corresponds to three different numerical methods, namely the MUSCL-Hancock scheme, the Godunov first-order upwind scheme and the Lax-Friedrichs scheme at time t=0.01 on 100 mesh cells are shown and compared with the reference solution (solid lines). The reference solutions in Fig. 10 are provided by

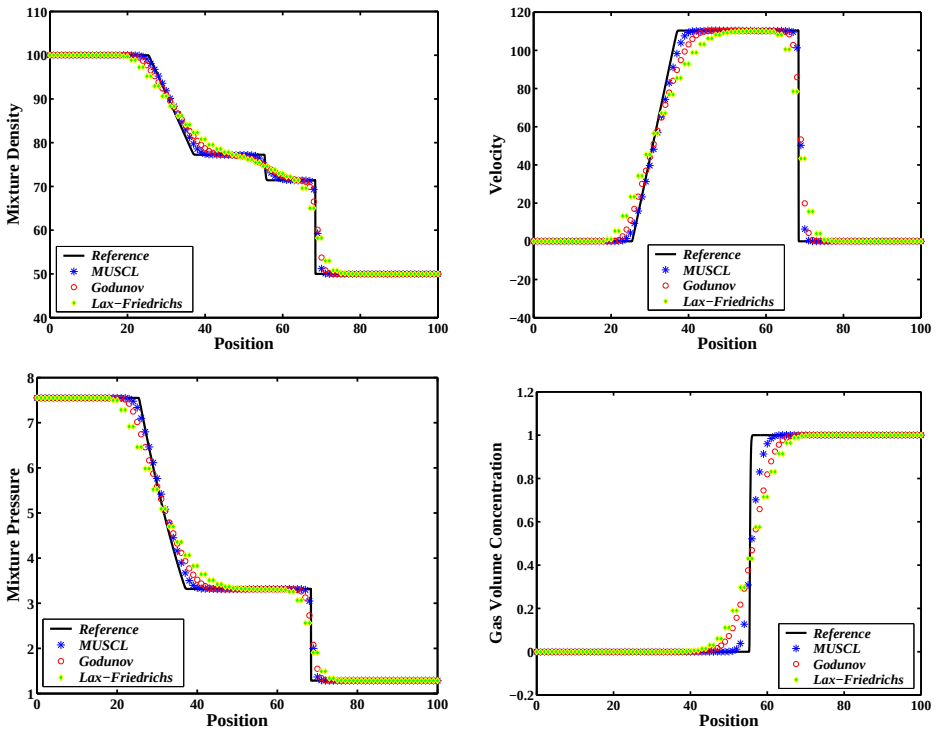

Figure 10: Comparison of numerical results (symbols) for test case 4.4 at time $t = 0.01$ from three numerical methods (MUSCL-Hancock and Godunov first-order upwind, with the HLL Riemann solver, and Lax-Friedrichs). Solid lines represent the reference solutions from the MUSCL-Hancock scheme with SUPERBEE limiter using the HLL Riemann solver on 4000 mesh cells. The top left and right panels show the mixture density (kg m^{-3}), velocity (m s^{-1}), respectively. While in the bottom left and right panels show the mixture pressure (Pa) and gas volume concentration, respectively.

the MUSCL-Hancock scheme together with the HLL Riemann solver using the SUPERBEE limiter on a mesh of 4000 cells. As seen from these plots, the TVD MUSCL-Hancock scheme solutions are very satisfactory and achieve sharper representation of the contact discontinuity when compared to the first-order Godunov and the Lax-Friedrichs methods. Also, the behaviour of the numerical solutions near shocks, contacts and rarefactions is the same for the three methods, but they differ in their ability to resolve the contact discontinuity. As it appears also, the comparison shows that the TVD MUSCL-Hancock scheme performs perfectly in view of the large variation in the values of the left and right states in gas volume concentration. In addition, Fig. 10 indicates that the MUSCL-Hancock scheme provides the best agreement with the reference solution whereas the first-order methods preserve diffusive character.

In Fig. 11 the same flow variables as in Fig. 10 are obtained by two different numerical methods (the MUSCL-Hancock scheme and the UCS approach) are compared with the reference solution. It can be seen that, the results (symbols) are in excellent agreement with the reference solutions (solid lines). However, it is found that the results provided

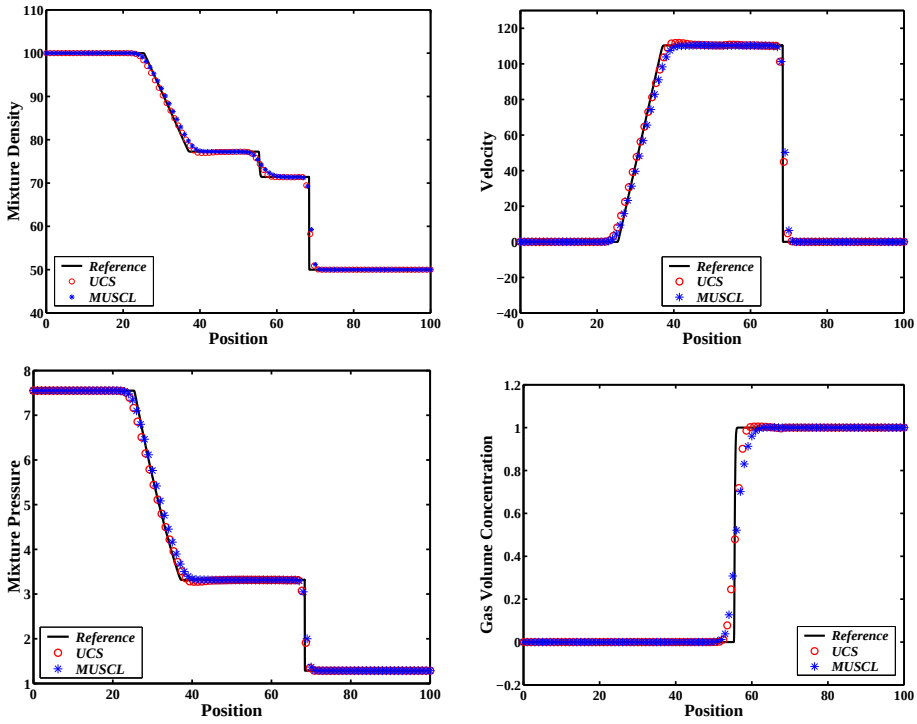

Figure 11: Numerical results in the volume wave propagation within two-phase gas-solid mixture at time $t=0.01$ (symbols). The computations have been obtained and compared by two different methods; that is, the MUSCL-Hancock scheme and the UCS approach on 100 mesh cells. The UCS results are obtained with CFL of 0.485. The solid lines show the reference solutions when the HLL Riemann solver is used in the TVD MUSCL-Hancock scheme. Results are corresponds to the mixture density (kg m^{-3}, top left), velocity (m s^{-1}, top right), the mixture pressure (Pa, bottom left) and gas volume concentration (bottom right).

by the TVD MUSCL-Hancock scheme are very satisfactory, oscillation-free and agree well with those predicted by the UCS approach. This validates the claim of oscillation-free of the MUSCL-Hancock scheme using the HLL Riemann solver. Based on the results and observations presented in Fig. 10 and Fig. 11, it can be noted that the mixture density profile change discontinuously across the middle wave. The reason for this is due primarily to the different values in the gas volume concentration on the left and right given initial conditions, see Table 2. Finally, to further illustrate the potential and capabilities of the numerical methods in the present paper, Fig. 12 shows numerical resolution for volume wave propagation within gas-solid mixture test case. We chose to display results for the mixture density and velocity using the two-dimensional version of the UCS numerical approach. We observe that both the rarefaction and shock waves are well simulated by the present numerical technique and free from any numerical problems. We also note that the rarefaction and shock waves are well captured using the UCS approach. In addition to that, the resolution profiles follow exactly the shape of the one-dimensional problem case. Overall, the results demonstrate support for this technique as a path towards resolution two-phase gas-solid mixture.

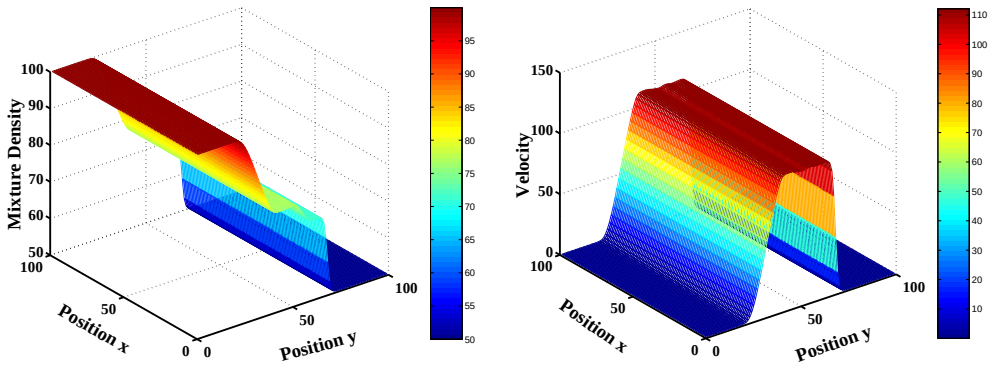

Figure 12: Volume wave propagation test case 4.4 for the two-dimensional two-phase gas-solid mixture. 3-D view of the mixture density (kg m^{-3}) and velocity (m s^{-1}) at time $t=0.01$ obtained with the UCS approach. The mesh contains 100×100 cells together with CFL$=0.485$.

5 Concluding remarks

This paper extends the range of previous work in the application of well-developed numerical methods to a well-defined mathematical model of compressible two-phase flow. As pointed out in [46], the mathematical and numerical study provides considerable support to the idea that fully hyperbolic and fully conservative character along with highly accurate and oscillation-free solutions on gas-solid mixtures are driven by thermodynamically compatible systems theory. This paper takes advantage of these facts and presents an innovative computations tool for the solution of thermodynamically compatible two-phase flow equations. As demonstrated in this paper, the proposed numerical approach using the HLL Riemann solver based upwind Godunov methods turns out to be surprisingly attractive. In this approach, a straightforward and natural extension of the well-known HLL Riemann solver is applied to solve the local Riemann problem for two-phase gas-solid mixture. The HLL Riemann solver is simple, efficient and enables the use of upwind methods of single-phase flow to solve the model equations. Furthermore, we have extended the Godunov first-order upwind scheme to two-phase gas-solid mixture. The TVD MUSCL-Hancock scheme has also been extended to the model equations.

To verify the accuracy of the proposed numerical methods, a series of test problems have been carried out. The obtained results show that the TVD MUSCL-Hancock scheme convergence has been achieved by the present approximate Riemann solver. They also show excellent agreement between the reference and numerical solutions, and they do match well with those provided solutions by other numerical methods. The results also demonstrate the ability of upwind methods to produce highly accurate resolution in smooth and discontinuous regions.

The recent development in two-phase flow phenomena requires new approaches for their mathematical and numerical modelling. In this paper we have shown that the use of the complete governing equations, rather than simplified as in most currently used

models, is emphasized for advanced modelling quality, which in essence does not cost much in computing efficiently and complexity. In order to elucidate various fundamental issues, the present paper is focused then on the most elementary approximate Riemann solver, involving the Mie-Grüneisen EOS. The next step, therefore, is dedicated to the development of exact and approximate Riemann solvers, such as the HLLC Riemann solver, for the two-phase gas-solid mixture in the framework of thermodynamically compatible systems theory with general equations of state. Future work in this step will rely and build upon the foundation in the present paper to involve one and multiple space dimensions two-phase gas-solid mixture using the Riemann solvers and Riemann-free solvers methods. Additional study in this direction also should concentrate on the interphase processes between the gas and solid phases. In another standard step forward is the inclusion of the relative velocity equation between the two phases. These issues seems potentially fruitful and currently pursuing by the present authors, and results will be presented elsewhere in the near future.

Acknowledgments

This paper was finalized during the stay of first author at the Center for Advanced Mathematical Sciences (CAMS), the American University of Beirut (AUB), Beirut, Lebanon. The authors acknowledge the financial support provided by CAMS/AUB. We also express our appreciation to Professor M. Darwish for his helpful and interesting discussions and meetings we have had.

References

[1] M. Baer and J. Nunziato, *A two-phase mixture theory for the deflagration-to-detonation transition (DDT) in reactive granular materials*, Int. J. Multiphase Flow, 12 (1986), pp. 861–889.

[2] J. W. Banks et al., *A high-resolution Godunov method for compressible multi-material flow on overlapping grids*, J. Comput. Phys., 223 (2007), pp. 262–297.

[3] V. Deledicque and M. V. Papalexandris, *An exact Riemann solver for compressible two-phase flow models containing non-conservative products*, J. Comput. Phys., 222 (2007), pp. 217–245.

[4] D. Drew and S. Passman, Theory of Multicomponent Fluids, (Applied Mathematical Sciences, Vol. 135), New York, Springer-Verlag, 1998.

[5] H. Enwald, E. Peirano and A.-E. Almstedt, *Eulerian two-phase flow theory applied to fluidization*, Int. Multiphase Flow, 22 (1996), pp. 21–66.

[6] H. A. Friis, S. Evje and T. Flatten, *A numerical study of characteristic slow-transient behavior of a compressible 2D gas-liquid two-fluid model*, Adv. Appl. Math. Mech., 1 (2009), pp. 166–200.

[7] S. K. Godunov and E. Romenski, Elements of Continuum Mechanics and Conservation Laws, Kluwer Academic/Plenum Publishers, 2003.

[8] H. Guillard and F. Duval, *A Darcy law for the drift velocity in a two-phase flow model*, J. Comput. Phys., 224 (2007), pp. 288–313.

[9] A. HARTEN, P.D. LAX AND B. VAN LEER, *On upstream differencing and Godunov-type schemes for hyperbolic conservation laws*, SIAM Rev., 25 (1983), pp. 35–61.
[10] X. Y. HU AND B. C. KHOO, *An interface interaction method for compressible multifluids*, J. Comput. Phys., 198 (2004), pp. 35–64.
[11] M. ISHII, Thermo-Fluid Dynamic Theory of Two-Phase Flow, Paris, Eyrolles, 1975.
[12] E. JOHNSEN AND T. COLONIUS, *Implementation of WENO schemes in compressible multicomponent flow problems*, J. Comput. Phys., 219 (2006), pp. 715–732.
[13] A. K. KAPILA ET AL., *Two-phase modeling of deflagrationto-detonation transition in granular materials: Reduced equations*, Phys. Fluids, 13 (2001), pp. 3002–3024.
[14] I. KATAOKA, *Local instant formulation of two-phase flow*, Int. J. Multiphase Flow, 12 (1986), pp. 745–758.
[15] J. J. KREEFT AND B. KOREN, *A new formulation of Kapila's five-equation model for compressible two-fluid flow, and its numerical treatment*, J. Comput. Phys., 229 (2010), pp. 6220–6242.
[16] Q. LIANG AND F. MARCHE, *Numerical resolution of well-balanced shallow water equations with complex source terms*, Adv. Water Res., 32 (2009), pp. 873–884.
[17] H. LUO, J. D. BAUM AND R. LÖÖHNER, *On the computation of multi-material flows using ALE formulation*, J. Comput. Phys., 194 (2004), pp. 304–328.
[18] E. A. LUKE AND P. CINNELLA, *Numerical simulations of mixtures of fluids using upwind algorithms*, Comput. Fluids, 36 (2007), pp. 1547–1566.
[19] N. C. MARKATOS AND D. KIRKCALDY, *Analysis and computation of three-dimensional, transient flow and combustion through granulated propellants*, Int. J. Heat Mass Trans., 26 (1983), pp. 1037–1053.
[20] H. NESSYAHU AND E. TADMOR, *Non-oscillatory central differencing for hyperbolic conservation laws*, J. Comput. Phys., 87 (1990), pp. 408–463.
[21] P. A. RAVIART AND L. SAINSAULIEU, *A nonconservative hyperbolic system modeling spray dynamics, Part I: solution of Riemann problem*, Math. Model. Methods Appl. Sci., 5 (1995), pp. 297–333.
[22] J. E. ROMATE, *An approximate Riemann solver for a two-phase flow model with numerically given slip relation*, Comput. Fluids, 27 (1998), pp. 455–477.
[23] E. ROMENSKI AND E. F. TORO, *Compressible two-phase flow models: two-pressure models and numerical methods*, Comput. Fluid Dyn. J., 13 (2004), pp. 403–416.
[24] E. ROMENSKI AND D. DRIKAKIS, *Compressible two-phase flow modelling based on thermodynamically compatible systems of hyperbolic conservation laws*, Int. J. Numer. Methods Fluids, 56 (2007), pp. 1473–1479.
[25] A. D. RESNYANSKYA AND N. K. BOURNE, *Shock-wave compression of a porous material*, J. Appl. Phys., 95 (2004), pp. 1760–1769.
[26] L. SAINSAULIEU, *Finite-volume approximation of two phase-fluid flows based on an approximate Roe-type Riemann solver*, J. Comput. Phys., 121 (1995), pp. 1–28.
[27] R. SAUREL AND R. ABGRALL, *A multiphase Godunov method for compressible multifluid and multiphase flows*, J. Comput. Phys., 150 (1999), pp. 425–467.
[28] D. W. SCHWENDEMAN, C. W. WAHLE AND A. K. KAPILA, *The Riemann problem and a high-resolution Godunov method for a model of compressible two-phase flow*, J. Comput. Phys., 212 (2006), pp. 490–526.
[29] R. K. SHUKLA, C. PANTANO AND J. B. FREUND, *An interface capturing method for the simulation of multi-phase compressible flows*, J. Comput. Phys., 229 (2010), pp. 7411–7439.
[30] H. STÄDTKE, Gasdynamic Aspects of Two-Phase Flow: Hyperbolicity, Wave Propagation Phenomena, and Related Numerical Methods, Weinheim, Wiley-VCH, 2006.

[31] H. B. STEWART AND B. WENDROFF, *Two-phase flow: models and methods*, J. Comput. Phys., 56 (1984), pp. 363–409.
[32] E. F. TORO, *Riemann-problem based techniques for computing reactive two-phase flows*, In: Dervieux, Larrouturrou, editors, Lecture Notes in Physics, Numerical Combustion, 351 (1989), pp. 472–481, Springer-Verlag.
[33] E. F. TORO, Riemann Solvers and Numerical Methods for Fluid Dynamics, A practical introduction, Berlin, Heidelberg, Springer-Verlag, 2009.
[34] S. A. TOKAREVA AND E. F. TORO, *HLLC-type Riemann solver for the Baer-Nunziato equations of compressible two-phase flow*, J. Comput. Phys., 229 (2010), pp. 3573–3604.
[35] R. TOUMA, *Central unstaggered finite volume schemes for hyperbolic systems: applications to unsteady shallow water equations*, Appl. Math. Comput., 213 (2009), pp. 47–59.
[36] I. TOUMI, AND A. KUMBARO, *An approximate linearized Riemann solver for two-fluid model*, J. Comput. Phys., 124 (1996), pp. 286–300.
[37] E. VALERO, J. DE VICENTE AND G. ALONSO, *The application of compact residual distribution schemes to two-phase flow problems*, Comput. Fluids, 38 (2009), pp. 1950–1968.
[38] B. VAN LEER, *Towards the ultimate conservative difference scheme V, a second-order sequel to Godunov's method*, J. Comput. Phys., 32 (1979), pp. 101–136.
[39] J. WACKERS AND B. KOREN, *A fully conservative model for compressible two-fluid flow*, Int. J. Numer. Methods Fluids, 47 (2005), pp. 1337–1343.
[40] B. WANG AND H. XU, *A method based on Riemann problem in tracking multi-material interface on unstructured moving grids*, Eng. Appl. Comput. Fluid Mech., 1 (2007), pp. 325–336.
[41] G. S. YEOM AND K. S. CHANG, *Numerical simulation of two-fluid two-phase flows by HLL scheme using an approximate Jacobian matrix*, Numer. Heat Trans. B, 49 (2006), pp. 155–177.
[42] D. ZEIDAN, A. SLAOUTI E. ROMENSKI AND E. F. TORO, *Numerical solution for hyperbolic conservative two-phase flow equations*, Int. J. Comput. Methods, 4 (2007), pp. 299–333.
[43] D. ZEIDAN, E. ROMENSKI, A. SLAOUTI AND E. F. TORO, *Numerical study of wave propagation in compressible two-phase flow*, Int. J. Numer. Methods Fluids, 54 (2007), pp. 393–417.
[44] D. ZEIDAN AND A. SLAOUTI, *Validation of hyperbolic model for two-phase flow in conservative form*, Int. J. Comput. Fluid Dyn., 23 (2009), pp. 623–641.
[45] D. ZEIDAN, *Applying upwind Godunov methods to calculate two-phase mixture conservation laws*, AIP Conference Proceedings, 1281 (2010), pp. 155–158.
[46] D. ZEIDAN, *Numerical resolution for a compressible two-phase flow model based on the theory of thermodynamically compatible systems*, Appl. Math. Comput., 217 (2011), pp. 5023–5040.
[47] H. W. ZHENG, C. SHU AND Y. T. CHEW, *An object-oriented and quadrilateral-mesh based solution adaptive algorithm for compressible multi-fluid flows*, J. Comput. Phys., 227 (2008), pp. 6895–6921.